Photosystem II

Dmitry Shevela, *Umeå University, Umeå, Sweden*
Jan F Kern, *Lawrence Berkeley National Laboratory, Berkeley, California, USA*
Govindjee Govindjee, *University of Illinois at Urbana-Champaign, Urbana, Illinois, USA*
John Whitmarsh, *University of Illinois at Urbana-Champaign, Urbana, Illinois, USA*
Johannes Messinger, *Umeå University, Umeå, Sweden and Uppsala University, Uppsala, Sweden*

Based in part on the previous versions of this eLS article 'Photosystem II' (2002, 2010).

Advanced article

Article Contents

Published online: 31st July 2021

Photosystem II (PSII) of plants, algae and cyanobacteria is a specialised protein complex that uses light energy to transfer electrons from water to plastoquinone, producing molecular oxygen and reduced plastoquinone. The PSII complex includes a peripheral antenna containing chlorophyll and other pigments to absorb light, a reaction centre that utilises the excitation energy transferred to it for charge separation, cofactors that stabilise the charge pair via electron transfer reactions, a Mn_4CaO_5 cluster that oxidises water, and a binding pocket where plastoquinone is reduced. The electrons and protons that PSII extracts from water are employed in the overall photosynthetic process for the reduction of CO_2, which provides the chemical energy for most life on Earth. PSII is the only known biological source of O_2 produced from water and is responsible for the molecular oxygen in the atmosphere.

Introduction

Oxygenic photosynthesis is the physical–chemical process by which plants, algae and certain bacteria use light energy to produce carbohydrates from carbon dioxide (CO_2) and water, resulting in the release of molecular oxygen into the atmosphere. The production of O_2 depends on photosystem II (PSII), a unique protein complex that removes electrons from water and transfers them to plastoquinone (PQ). Fossil evidence and genome analysis indicate that PSII-containing organisms emerged between 2.4 and 3.5 billion years ago, resulting in the conversion of the Earth's atmosphere from a mildly reducing anaerobic state to the O_2-rich air surrounding us today (Catling and Zahnle, 2020). The release of oxygen into the atmosphere by PSII enabled the evolution of oxidative respiration, which has had a profound impact on the diversity of life on our planet. **See also**: **Earth: Changes Through Time**; **Evolution of Photosynthesis**; **Photosynthesis**

The light-driven reactions of oxygenic photosynthesis take place in the photosynthetic thylakoid membranes of chloroplasts and cyanobacteria (**Figure 1a**), while the light 'independent' CO_2 fixation occurs in the stroma (in chloroplasts) or the cytoplasm (in cyanobacteria) surrounding the thylakoids. The thylakoid membrane encloses an inner aqueous volume, the lumen. Chloroplasts, which are the photosynthetic 'engines' of plants and algae, originated from oxygenic bacteria that were engulfed by a eukaryotic nonphotosynthetic organism.

The thylakoid membranes contain three major protein complexes that include all the components needed for the light-powered electron transfer chain from water to nicotinamide–adenine dinucleotide phosphate ($NADP^+$) (**Figure 1b**,**c**). PSII is the starting point of this chain; it employs light energy to extract electrons from water molecules, a process that allows oxygenic photosynthesis to utilise water as a resource for electrons and protons for CO_2 fixation. PSII transfers these electrons to a mobile carrier, PQ, which in its 2-electron reduced form, plastohydroquinone (PQH_2), transfers the two electrons to the cytochrome (Cyt) b_6f complex. In chloroplasts, Cyt b_6f transfers the electrons onto the one-electron carrier plastocyanin (PC), which then transfers the electrons to photosystem I (PSI). PSI performs another light reaction, simultaneous to that of PSII, that produces enough reducing power for converting $NADP^+$ to NADPH. Through a mechanism known as the Q-cycle, electron transfer from PSII to PC is coupled to the transfer of two protons per electron from the stroma/cytoplasm to the lumen of the thylakoid membrane. The cyclic electron transfer indicated in **Figure 1b** becomes important under conditions where carbon fixation cannot keep up with the electron delivery by the light reactions and contributes to producing ATP (see below) and in protecting the electron transfer chain

eLS subject area: Biochemistry

How to cite:
Shevela, Dmitry; Kern, Jan F; Govindjee, Govindjee; Whitmarsh, John; and Messinger, Johannes. *Photosystem II*, eLS, **Vol 2**: 1–20, 2021.
DOI: 10.1002/9780470015902.a0029372

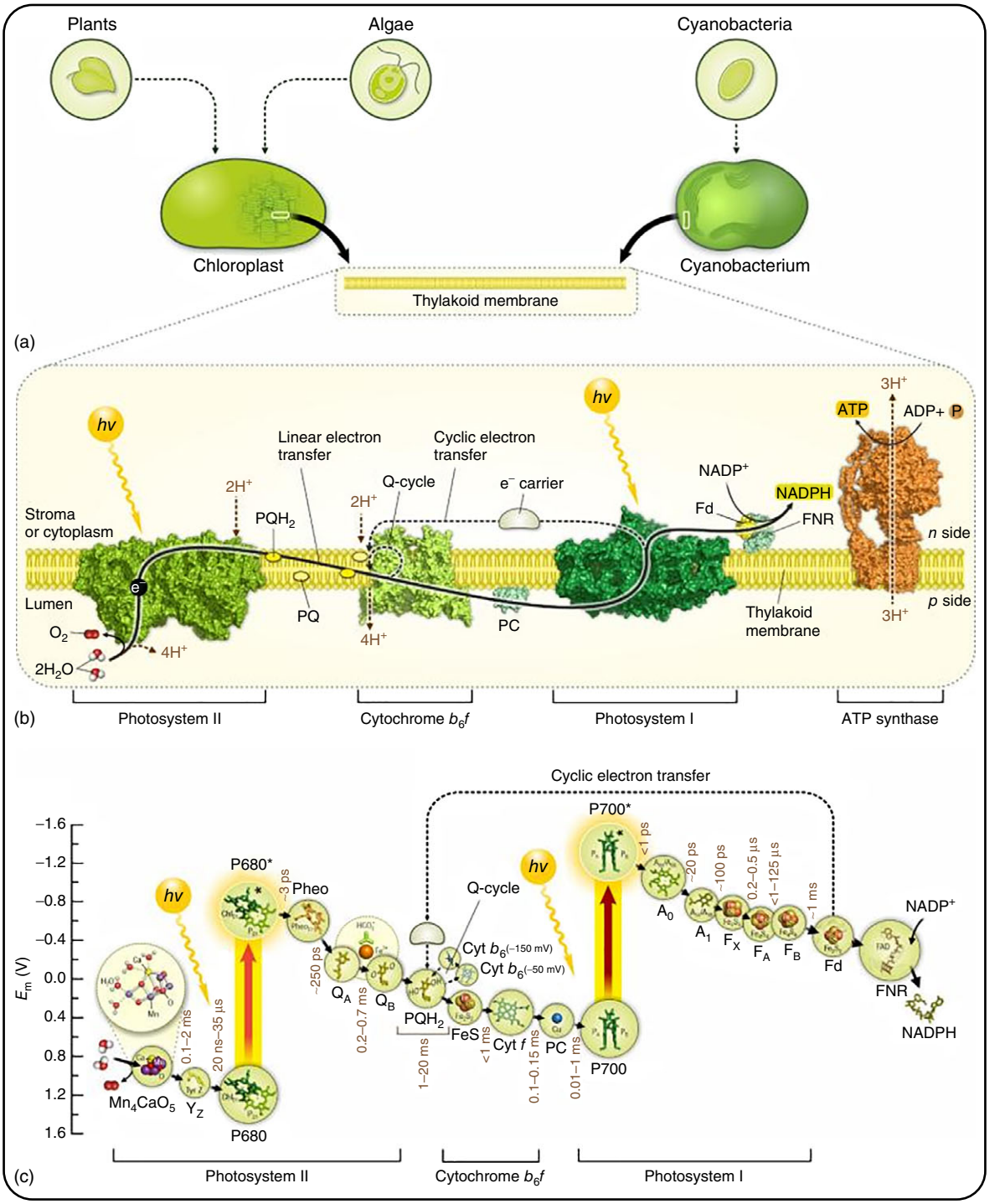

from damage. **See also**: **Chlorophyll: Structure and Function**; **Photosystem I**; **Plant Chloroplasts and Other Plastids**

A fourth complex in the thylakoid membrane, the ATP synthase (**Figure 1b**), utilises the proton electrochemical potential across this membrane for making ATP from ADP and inorganic phosphate (P_i). In addition to oxygen, the products of the light-driven electron and proton transport reactions are NADPH and ATP, which together provide the free energy needed for the reduction of CO_2 and the synthesis of carbohydrates. **See also**: **Algal Chloroplasts**; **Photophosphorylation**; **Photosynthesis: The Calvin Cycle**; **Photosynthetic Carbon Metabolism**; **Rubisco**; **Mitchell, Peter Dennis**

Figure 1 (a) Location of the photosynthetic thylakoid membrane in higher plants, algae and cyanobacteria. (b) A schematic view of photosynthetic protein complexes embedded in the thylakoid membrane. Except for ATP synthase (extreme right), these complexes bind the redox components (shown in panel c) required for the light-dependent *linear electron transfer* (see the long black bold arrow) from water (bottom left) to $NADP^+$. Under some conditions, electrons on the electron acceptor side of Photosystem I (PSI) cycle back towards Cytochrome b_6f (Cyt b_6f) complex and then again towards PSI, thus performing a *cyclic electron transfer* (dashed arrow). The *Q-cycle* in the Cyt b_6f increases the number of protons pumped across the membrane, per electron transferred. Note that PSII, Cyt b_6f complex, PSI, and ATP synthase are not necessarily in 1:1:1:1 ratio. These complexes may be physically distant from each other in the thylakoid membrane, and their functional connection is accomplished through diffusible PQ (between PSII and Cyt b_6f) or by PC (between Cyt b_6f and PSI). (c) The Z scheme for photosynthetic electron transport from water to $NADP^+$. The vertical scale shows the equilibrium midpoint redox potential (E_m, at pH 7) of the electron transport components. Approximate electron transfer times are shown for most of the reactions. Abbreviations: Mn_4CaO_5, manganese-calcium-oxygen complex; Y_Z, redox-active tyrosine (Tyr Z); P680, primary electron donor of PSII that includes the chlorophyll *a* (Chl *a*) molecules P_{D1}, P_{D2}, Chl_{D1}, and Chl_{D2}; only Chl_{D1} and P_{D1} are shown; P700, primary electron donor of PSI formed by the Chl *a* molecules P_A and P_B; $P680^*$ and $P700^*$ are the first singlet excited states of P680 and P700; Pheo, pheophytin of which $Pheo_{D1}$ is the primary electron acceptor of PSII; Q_A and Q_B, primary and secondary plastoquinone electron acceptors; PQ, mobile plastoquinone molecules; FeS, Rieske iron-sulfur protein; Cyt *f*, cytochrome *f*; PC, plastocyanin, a mobile copper protein; A_0, primary electron acceptor of PSI (a special pair of Chl *a* molecules, A_{0A} and A_{0B}); A_1, pair of phylloquinone (vitamin K) molecules, A_{1A} and A_{1B}; F_X, F_A, and F_B, bound iron-sulfur clusters of PSI; Fd, ferredoxin, and FNR, ferredoxin-$NADP^+$ reductase. Complexes and cofactors shown in Panels b and c were generated using coordinates of the following PDB codes: 1AG6, 1VF5, 1SM4, 2MH7, 2GIM, 3ARC, 3W5U, 3WU2, 4Y28, 5L8R, 6B8H, and 6W1O. Phytol tails of Chls and Pheo and the isoprenyl chains of the quinones are not shown. (b, c) Modified from D. Shevela and G. Govindjee (doi.10.13140/RG.2.2.22936.14081 and doi 10.13140/RG.2.2.22936.14081).

As described above, two distinct light reactions (PSII and PSI) provide the energy for the uphill electron transfer from water to $NADP^+$. The cofactors involved and their respective electrochemical midpoint potentials, as well as the approximate times for electron transfer reactions, are shown in **Figure 1c**. Note that after each light-induced charge separation a significant amount of energy is rapidly converted to heat energy and is therefore not able to contribute to photosynthetic energy conversion. Although this two reaction centre energy profile (historically known as the *Z-scheme*; see Govindjee *et al*., 2017) may appear wasteful, it ensures high quantum efficiency for the coupling of the super-fast (1–3 ps) one electron charge separation reactions with the nine orders of magnitude slower (1–20 ms) multielectron, multiproton chemical reactions. We note that part of the energy conversion during this stabilisation process is stored by moving protons across the membrane that contribute to ATP synthesis. The conversion of solar light energy to chemical energy in biomass can be as high as 3% for microalgae and cyanobacteria grown in bioreactors and 0.3–1% for plants (Blankenship *et al*., 2011; Ort *et al*., 2015).

Below, we describe the structure and function of PSII without discussing the experimental results that underlie our knowledge. The references were selected to provide entry points to the scientific literature describing progress in understanding this ubiquitous enzyme, whose emergence 3 billion years ago was a seminal event in evolution.

Overview of photosystem II function

PSII uses light energy to drive two chemical reactions: the oxidation of water (reaction I) and the reduction of PQ (reaction II) (Renger and Renger, 2008).

$$2H_2O \rightarrow O_2 + 4e^- + 4H_{lumen}{}^+ \quad \text{(I)}$$

$$PQ + 2e^- + 2H_{stroma}{}^+ \rightarrow PQH_2 \quad \text{(II)}$$

The absorption of light (photons) in the light-harvesting pigment–protein complexes of PSII creates excited electronic states in Chl molecules, within femtoseconds (10^{-15} s). Once this excitation energy reaches the reaction centre, P680 ($Chl_{D1}/P_{D1}/P_{D2}/Chl_{D2}$) and $Pheo_{D1}$ (**Figure 2**), P680* is formed (**Figure 1c**). P680* then transfers one electron to $Pheo_{D1}$. This primary charge separation, which occurs within 3 ps or less (Mamedov *et al*., 2015), is subsequently stabilised to allow reactions I and II, which occur in the 1–20 ms range. This long stabilisation of the initial charge separation is achieved by a series of electron transfer reactions that increase the distance for charge recombination and reduce the energy difference between the redox cofactors involved, which are the bound PQ molecules Q_A and Q_B on the electron acceptor side of PSII, as well as the tyrosine side chain Y_Z and the Mn_4CaO_5 cluster on the electron donor side of PSII (**Figure 2**). Each light-induced charge separation in PSII drives the transfer of one electron from the Mn_4CaO_5 cluster to Q_B. Thus, four photochemical reactions are required to remove four electrons from two water molecules, which results in the production of one molecule of oxygen and the release of four protons into the inner water phase (the lumen) of the photosynthetic membrane (**Figure 2**). The four electrons extracted from two water molecules sequentially reduce two PQ molecules to PQH_2. The protons for PQ reduction are taken up from the stromal (or cytoplasmic) water phase.

The quantum efficiency of PSII can reach values of 90%, while its solar-to-chemical energy efficiency has been estimated to be ~16% under optimal conditions (Dau and Zaharieva, 2009). The turn-over frequency of PSII is limited by the PQH_2/PQ exchange at the (electron) acceptor side to about 50 O_2 s^{-1} or 200 electrons s^{-1} (Lee and Whitmarsh, 1989). In full sunlight, each PSII can produce about 100 000 O_2 molecules (turnover number) before it needs to be repaired. Interestingly, it is not the Mn_4CaO_5 cluster that breaks down, but the D1 protein becomes damaged.

Present synthetic catalysts require rare and expensive metals such as ruthenium or iridium to achieve comparable water oxidation activities as PSII. Chemists are thus fascinated by how the base metals Mn and Ca are activated in PSII to work as a highly efficient water oxidation catalyst. This activation may, in part, be due to the open and flexible structure of the Mn_4CaO_5 cofactor, the tuning of electronic spin states for low energy O—O bond formation via oxo-oxyl radical coupling, and the H-bonding network for efficient proton removal and controlled water access via channels.

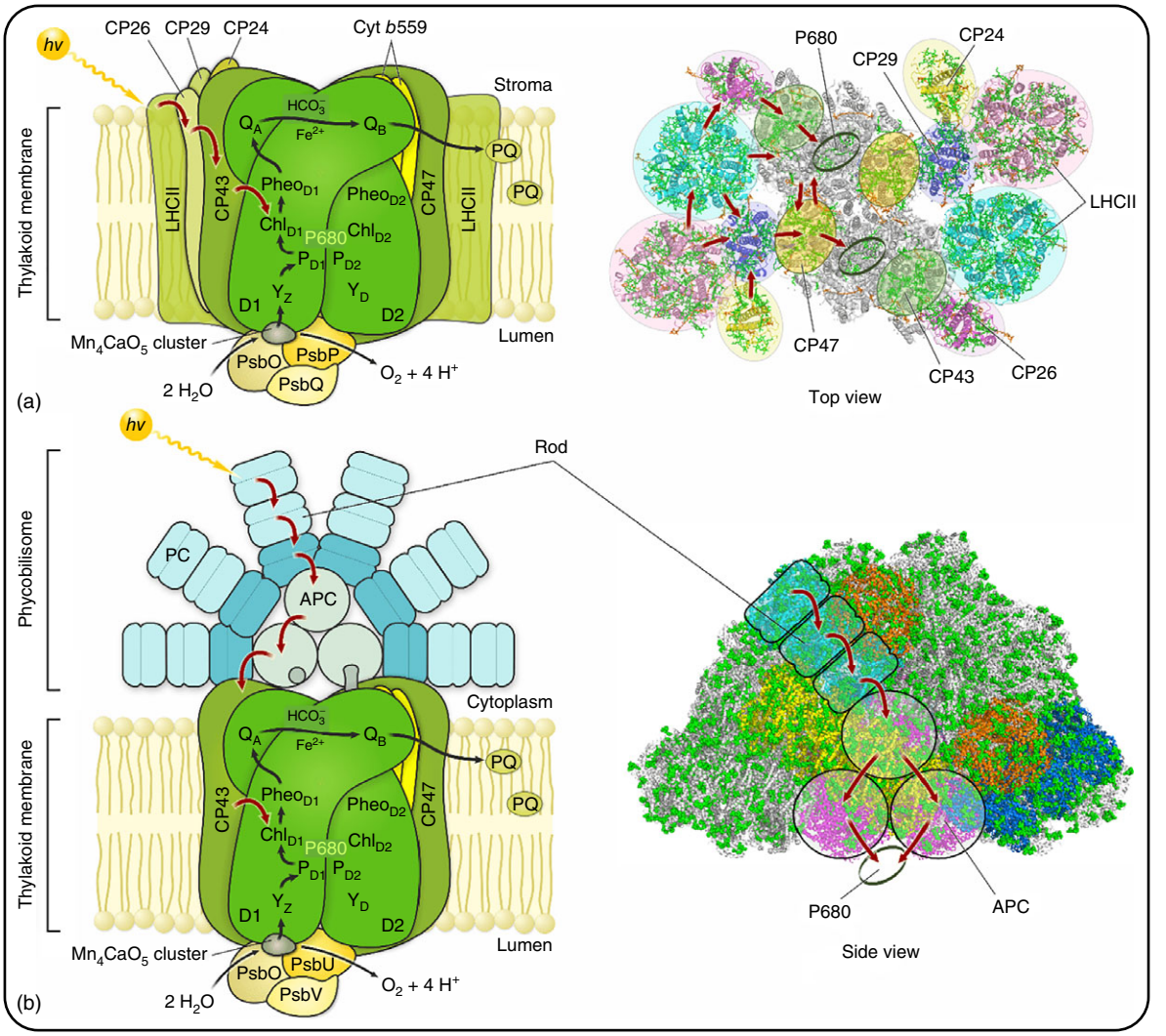

Figure 2 Schematic representation of proteins and electron transfer cofactors of photosystem II (PSII) and the connected antenna system for (a) higher plants and green algae, and (b) cyanobacteria. D1 and D2 are the reaction centre proteins of PSII that bind the electron transfer cofactors, whereas CP43 and CP47 bind Chl *a* molecules and function as inner antenna of PSII. The Mn_4CaO_5 cluster is stabilised by three extrinsic proteins, which differ in plants and cyanobacteria, except for the PsbO protein. While higher plants and algae have additional integral membrane proteins for light-harvesting (LHCII) (a), PSII in cyanobacteria utilises phycobilisomes to capture light energy (b). The phycobilisomes are anchored to the cytoplasmic side of the PSII complex and are comprised of phycocyanins, PCs, and allophycocyanins, APCs. Parts of the figure were generated by using the coordinates from PDB codes 5XNL and 6KGX. Please note, that the coordinates for phycobilisomes (PDB ID: 6KGX) originate not from a cyanobacterium but from the red alga *Porphyridium purpureum*. Currently, this is the only available entire phycobilisomes structure, which is supposed to be similar with cyanobacterial phycobilisomes. For abbreviations see the legend of **Figure 1**.

Organisation, Composition and Structure

There is a remarkable similarity in the structure and function of PSII in higher plants (Su *et al*., 2017), different algae (green, red) and cyanobacteria (Kern *et al*., 2018; Umena *et al*., 2011). PSII shares several structural features with PSI and (anoxygenic) bacterial reaction centres, indicating ancient evolutionary links. By contrast, the structures of the light-capturing antenna systems in various photosynthetic systems are quite different (**Figure 2**), indicating multiple origins. **See also**: **Evolution of Photosynthesis**

PSII is embedded in the thylakoid membranes of chloroplasts and cyanobacteria (**Figure 1a**). In chloroplasts, the thylakoids have both stacked (grana) and nonstacked (stroma) regions, with most of the PSII in the grana, and virtually all the PSI in the stroma. In the grana, the PSII complexes are densely packed, with 150–250 Å centre-to-centre distance. In prokaryotes, the photosynthetic membranes do not form stacked membranes, and the PSII and PSI complexes are intermixed.

Functionally, PSII can be divided into a reaction centre core and a surrounding light-harvesting antenna (**Figure 2a**,**b**). The antenna consists of protein complexes that spatially organise and spectrally tune the light-absorbing molecules: chlorophylls or phycobilins, and other accessory pigments. All these pigments operate in concert to capture photons and transfer the excitation energy to the PSII reaction centres where the primary charge separation occurs. In most eukaryotic organisms (e.g., higher plants and green algae), the light-harvesting complexes (LHCs) are membrane integral pigment–proteins. They are organised as an inner antenna system tightly connected to the reaction centre, and a peripheral antenna system known as light-harvesting complex II (LHCII) (**Figure 2a**). In red algae (eukaryote) and in most cyanobacteria (prokaryote), the outer LHCs are attached to the cytoplasmic site of PSII. These phycobilisomes contain phycobilin pigments rather than chlorophylls to capture light (**Figure 2b)**.

Currently, the best structures of PSII have 1.85–1.9 Å resolution when obtained at very low temperatures (Umena *et al*., 2011), and ~2.0 Å resolution when the data were collected at room temperature (Ibrahim *et al*., 2020; Kern *et al*., 2018). PSII complexes are composed of more than 20 different proteins, of which 17 are integral membrane proteins (**Figure 3a**,**b**) (Shi *et al*., 2012). In addition, several small membrane intrinsic proteins are found in plants, but not in cyanobacterial PSII. Furthermore, several additional proteins are present in sub-stoichiometric amounts as they are involved in the assembly and repair of PSII. **Table 1** gives a complete overview of the PSII proteins, their encoding genes, molecular weights, and putative function. **See also**: **Chloroplast Genome**

While the inner antenna is formed by the CP43 and CP47 proteins, the D1 and D2 proteins comprise the core of PSII. They bind all the cofactors necessary for photochemical charge separation, the subsequent electron transfer steps, as well as Reactions I and II. These cofactors include the Mn_4CaO_5 cluster, the tyrosine Y_Z (or Tyr_Z), a chlorophyll dimer (P_{D1} and P_{D2}), a monomeric chlorophyll (Chl_{D1}), a pheophytin ($Pheo_{D1}$) and two differently bound PQ molecules (Q_A and Q_B) (**Figures 2** and **3a**). Most of these cofactors are located on the 'left (D1)' branch of the seemingly symmetric cofactor arrangement. Other cofactors – such as Chl_{D2}, carotenoids, Y_D and Cyt *b*559 – are also redox active, but donate electrons only when the electron transfer via the Mn_4CaO_5 cluster and Y_Z is blocked. These cofactors have been proposed to have protective roles in PSII. (**Figure 3b**; **Table 1**).

The symmetry of the two branches is broken in part by the position of the Mn_4CaO_5 cluster at the luminal side. The Mn_4CaO_5 cluster is connected to the central chlorophylls via the redox active tyrosine Y_Z (**Figure 3a**) that transfers electrons from the Mn_4CaO_5 cluster to $P680^+$. The binding of the Mn_4CaO_5 cluster is stabilised by three peripheral (extrinsic) proteins. Interestingly, they differ between species: plant PSII contains PsbO (33 kDa), PsbP (23 kDa) and PsbQ (16 kDa), while cyanobacterial PSII has PsbO (33 kDa), PsbU (12 kDa) and PsbV (Cyt *c*550) (see **Figure 2a**,**b**) (Roose *et al*., 2016).

The Mn_4CaO_5 cluster is ligated by amino acids from the D1 protein and the inner antenna protein CP43 (**Figure 4**; **Table 1**). Each Mn atom in the cluster is connected to the other metals by two or three di-μ oxo bridges. The overall structure can be described as an open cube formed by 3 Mn ions and 1 Ca ion with one more separate Mn, Mn4, connected via two oxo bridges to the Mn_3Ca unit. The cluster is coordinated to the protein by one histidine residue (D1-His332) and five carboxylate groups: D1-Asp170, D1-Glu189, D1-Glu333, CP43-Glu354 as well as the C-terminus of the D1 protein, D1-Ala344. The carboxylates always bridge two metals of the cluster and the coordination sphere of the metal cluster is completed by four water molecules, W1 and W2 bound to Mn4, and W3 and W4 bound to the Ca ion (**Figure 4b**,**c**) (Kern *et al*., 2018; Umena *et al*., 2011). The Mn_4CaO_5 cluster is embedded in a larger hydrophilic pocket that is filled by ~20 water molecules, which form an intricate hydrogen-bonding network. Three main channels connect this pocket with the lumen (**Figures 3b** and **4a**). Based on their diameter, polarity, and structural changes during enzyme turnover the O4 and Cl1 channels are considered to be likely involved in proton transfer, while the water access to the Mn_4CaO_5 cluster is suggested to occur via the O1 or the Cl1 channel, with the O1 channel showing a higher mobility of water molecules (Ibrahim *et al*., 2020). Pathways and channels exist also at the Q_B site for proton transfer from the outer water phase, as well for the access of quinones to the Q_B binding site (Ho, 2012).

The pathway and rate of electron transfer between the cofactors in the electron transport chain of PSII (**Figure 3a**) must be controlled for efficient operation. Key factors controlling electron transfer from one redox site to another are the distance and relative orientation of the components (Moser *et al*., 1992), which are determined by the protein scaffolding of the complex. Another factor is protein dynamics, which appears to play an important role in the stabilisation of the primary charge separation and other reactions within PSII.

Light Capture: The Antenna System

In all oxygenic photosynthetic organisms, the light reactions in PSII and PSI begin with the capture of light (*photons*) by chromophores (*pigments*) located in antenna proteins organised into *light-harvesting complexes* (LHCs). Depending on the organism, the pigments include chlorophyll *a*, other chlorophylls, carotenoids, or phycobilins. These are bound to the LHCs in specific geometric arrangements. Most of these pigments act as antenna molecules.

In addition to the core antenna formed by CP47 and CP43, PSII of plants and green algae is connected to additional antenna complexes, known as LHCII, and minor complexes that include chlorophyll–protein complexes with masses of 24 and 26 kDa (**Figure 2a**). The LHCII is a trimer, with each subunit binding eight molecules of chlorophyll *a*, six of chlorophyll *b,* and four of carotenoids. CP43 and CP47 contain only chlorophyll *a* (Müh and Zouni, 2020). The major LHCs of PSII in cyanobacteria, red and glaucophyte algae are the *phycobilisomes* that are made of the *phycobilins*. In contrast to LHCII, phycobilisomes are attached to the cytoplasmic surface of PSII and are not integral to the membrane (see **Figure 2b**, and a review by Green (2019)). **See also**: **Chlorophyll-Binding Proteins**

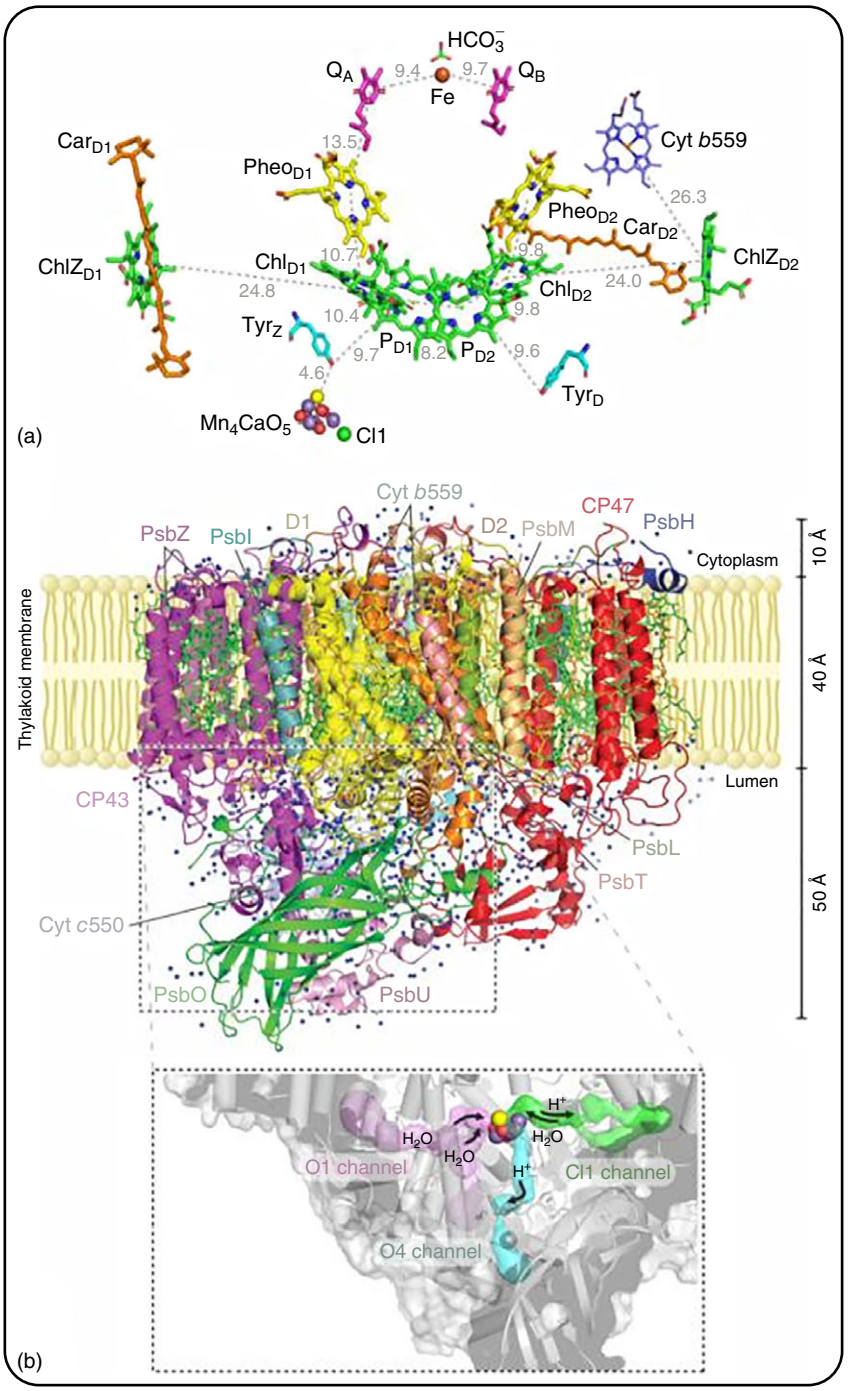

Figure 3 Structure of the photosystem II (PSII) complex from a thermophilic cyanobacterium *Thermosynechocuus elongatus*. (a) Redox-active cofactors in the reaction centre; this view is along the membrane plane, with the cytoplasm at the top and the lumen at the bottom. Centre-centre distance of the cofactors is given in Å, except for the redox-active tyrosines, Tyr_Z (Y_Z) and Tyr_D (Y_D), where edge-edge distances are given. The catalytic site of water oxidation is the Mn_4CaO_5 cluster (magenta, yellow and red spheres). Cofactors are shown in green (chlorophylls), orange (carotenoids), blue (heme) and yellow (lipids), while water molecules are shown as blue dots. (b) Structure of the entire PSII complex (monomer) embedded in a schematic thylakoid membrane, with the view direction along the membrane plane. Protein subunits are shown as a cartoon and are labelled in the figure. The bottom of the figure shows a zoomed-in view of the luminal extension of PSII. This highlights the three main channels that connect the Mn_4CaO_5 cluster (shown as spheres) with the lumen. These channels are postulated to transport H_2O and H^+s between the lumen and the Mn_4CaO_5 cluster. The figure was generated by using the coordinates from PDB code 6W1O.

Table 1 Photosystem II genes, proteins and putative roles (excluding external antenna proteins)

Gene[a]	Protein	Mass (kDa)[b]	Integral/ peripheral[c]	Function/comments
psbA (c)	D1	39	I (5)	D1 and D2 form the reaction centre core, binding most of the PSII electron transport components, provides ligands to the OEC, binds Q_B
psbB (c)	CP47	56	I (6)	Binds antenna Chls *a*, carotenoids,
psbC (c)	CP43	47	I (6)	Binds antenna Chls *a*, carotenoids, provides a ligand to the OEC
psbD (c)	D2	39	I (5)	D2 and D1 form the reaction centre core, binding most of the PSII electron transport components, binds Q_A
psbE (c)	*α* subunit Cyt *b559*	9.3	I (1)	Binds *b*-heme, maybe involved in photoprotection and secondary electron transfer
psbF (c)	*β* subunit Cyt *b559*	4.5	I (1)	Binds *b*-heme, maybe involved in photoprotection and secondary electron transfer
psbG	PsbG	?	I (1)	Found in diatoms (*C. gracilis*), connection to outer antenna
psbH (c)	PsbH	7.8	I (1)	Can be phosphorylated in plants, interacts with CP47, in contact with 3 Chls, possibly involved in PSII repair and electron transport at acceptor side
psbI (c)	PsbI	4.2	I (1)	Stabilisation and assembly of complex, dimer formation (cyanobacteria), connection to outer antenna (plants)
psbJ (c)	PsbJ	4.2	I (1)	Influences plastoquinone (Q_B) exchange and electron flow on acceptor side
psbK (c)	PsbK	4.3	I (1)	Stabilisation of complex
psbL (c)	PsbL	4.5	I (1)	Influences plastoquinone (Q_A) binding and electron flow on acceptor side, stabilises dimerisation
psbM (c)	PsbM	4.0	I (1)	Stabilises monomer-monomer contact in the PSII dimer
psbO (n)	PsbO, 33 kDa protein, manganese stabilising protein (MSP)	27	P (0)	Stabilises Mn cluster, might be involved in Ca^{2+} association with the OEC, proton transfer away from the OEC, might help to provide contact between dimers of PSII in cyanobacteria
psbP (n)	PsbP	20	P (0)	Eukaryote specific, cyanobacterial counterpart (CyanoP) of unclear role, not located in structures
psbQ (n)	PsbQ	17	P (0)	Eukaryote specific, counterpart of PsbQ' found in red algae and diatoms, in cyanobacteria CyanoQ present but not located in structures
psbR (n)	PsbR	10	P (0)	Eukaryote specific supports binding of extrinsic subunits in plants
psbS (n)	PsbS	21	I (4)	Eukaryote specific, involved in nonphotochemical quenching
psbT (c)	PsbT, $PsbT_c$	3.8	I (1)	Stabilises Q_A-binding site, supports dimerisation, assembly
psbT (n)	$PsbT_n$	3.2	P (0)	Eukaryote specific/unknown function
psbU	12 kDa protein	12	P (0)	Present in cyanobacteria, diatoms and red algae
psbV	Cyt *c550*, 17 kDa protein	17	P (0)	Binds heme, present in cyanobacteria, diatoms and red algae, optimises oxygen evolution activity
psbW (n)	PsbW	6	I (1)	Not found in cyanobacteria, binds to CP43, close contact to PsbI, interacts with PsbO, maybe interacting with outer antenna
psbX (c)	PsbX	4.1	I (1)	Involved in quinone turnover at Q_B site
psbY (c)	PsbY	4.7	I (1)	Closely associated with Cyt *b*559 in cyanobacteria, not clear if present in stoichiometric amounts in plants
psbZ (c)	PsbZ	11	I (2)	Connection to outer antenna
ycf12 (c)	Psb30, Ycf12	5	I (1)	Photoprotection, interaction with Cyt *b*559
psb31	Psb31	17	P(0)	Found in diatoms (*C. gracilis*), bound to CP47 and D2
psb34	PsbN	4.7	I(1)	Found in diatoms (*C. gracilis*) and red algae

Chl, chlorophyll; Cyt, cytochrome; OEC, oxygen-evolving complex; I, integral; P, peripheral.

[a]For eukaryotic organisms, the letter in parentheses indicates whether gene is nuclear (n) or chloroplast (c) encoded.

[b]Mass is calculated from amino acid sequence.

[c]Number of transmembrane helices is given in parentheses.

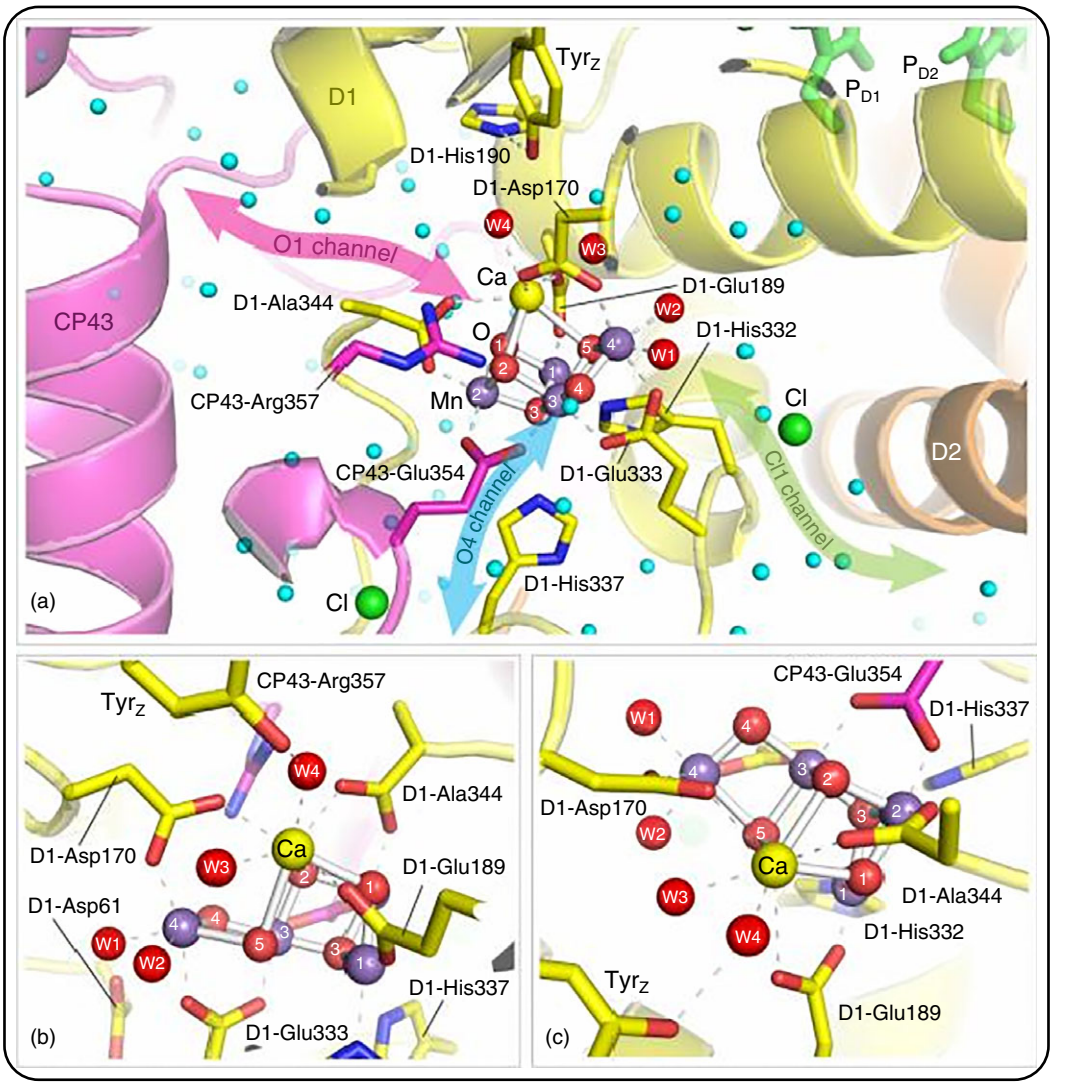

Figure 4 The catalytic site of water oxidation in photosystem II (PSII). (a) Structural model for the metal ions and amino acid ligands (three-letter codes) of the Mn_4CaO_5 cluster, the redox-active tyrosine Tyr_Z (D1-Tyr161) and the chlorophylls P_{D1} and P_{D2}; the view is along the membrane with the lumen at the bottom and the cytoplasm at the top. The surrounding protein is shown in light yellow (D1), orange (D2) and magenta (CP43). Mn (purple), Ca^{2+} (yellow), Cl^- (green) ions and oxygens (red) are shown as spheres, ligating to amino acids. Water molecules, located in the crystal structure, are shown as cyan spheres. Suggested water and proton channels are indicated by broad arrows. The nitrogen and oxygen atoms of the amino acid ligands are coloured in blue and red, respectively; the carbon atoms are coloured depending on the subunit the amino acid belongs to yellow for D1 and magenta for CP43. (b) and (c) The Mn_4CaO_5 cluster and its direct amino acid ligands shown in two different orientations, either along the membrane plane (b) or looking downwards from the membrane plane in the direction of the lumen (c). Mn atoms are numbered 1–4, bridging oxygens as 1–5, and metal bound waters as W1–W4. The figure was generated by using the coordinates of the PDB code 6W1O.

The major light-absorbing pigment in plants and many algae is chlorophyll, a green pigment that strongly absorbs blue and red light (**Figure 5b**). The absorption spectrum of chlorophyll (shown on the right in **Figure 5b**) has two dominant peaks, corresponding to two major singlet excited states (S_1 and S_2). The higher excited state S_2 corresponds to the absorption band in the blue part of the spectrum, while the lower excited state S_1 corresponds to the absorption band in the red part of the spectrum. The excited state S_2 of the chlorophyll molecule is short lived and decays in $\sim 10^{-13}$ s to the excited state S_1, whereby the excess energy is dissipated as heat energy. The excited state S_1 is also created by absorption of red light (**Figure 5b**).

The fate of the S_1 excited state is determined by the structure and composition of the LHCs as well as the state of the electron and proton transfer reactions of the photosynthetic apparatus. Because of the proximity of other antenna pigment molecules with the same or similar electronic energy levels, the excited singlet state energy has a high probability of being transferred

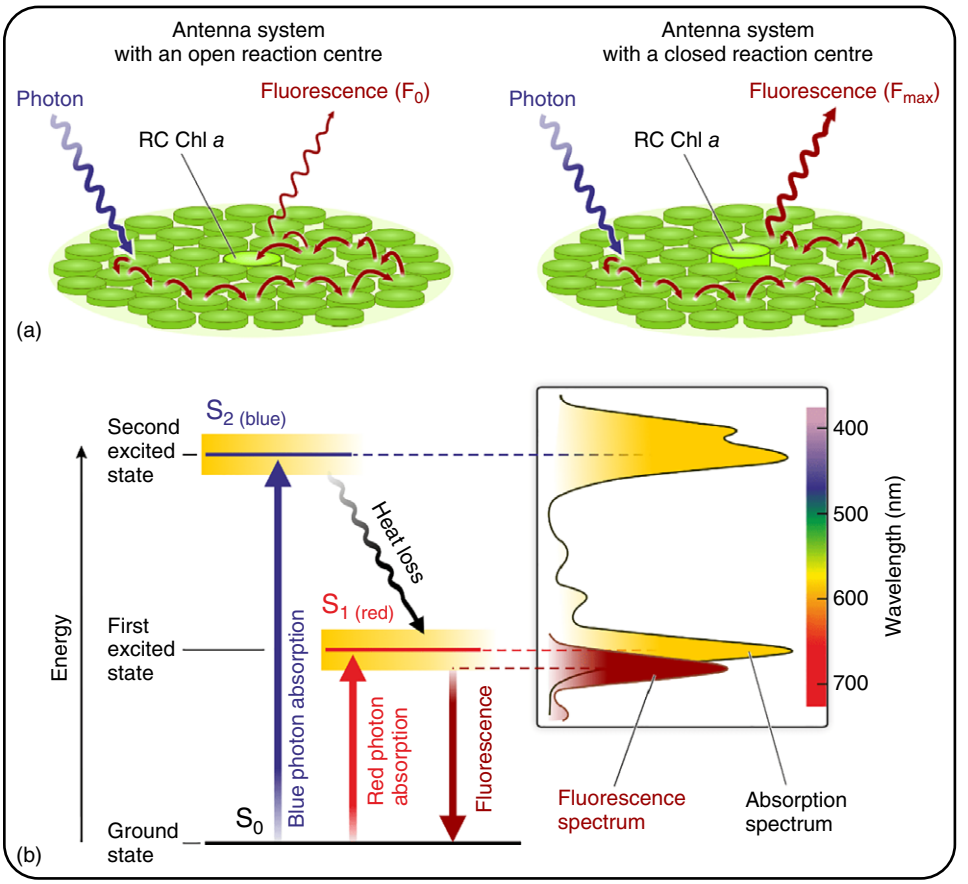

Figure 5 (a) Schematic representation of excitation energy transfer (red arrows) from one chlorophyll (Chl) molecule to another in a 'generic' light-harvesting-complex-type antenna system of higher plants. Green discs represent Chl *a* and *b* molecules; the pale green disc in the middle represents the reaction centre, which is open on the left and closed on the right (visualised by its greater thickness). When the reaction centre is open (a, left), most energy is used for charge separation, and the system emits minimal Chl *a* fluorescence (labelled as F_0); when the reaction centre is closed (a, right), Chl *a* fluorescence is maximal (F_{max}). (b) A simplified 'Jablonski-Perrin' diagram (named after Aleksander Jablonski and Jean Perrin) of the energy levels of a Chl molecule with spectral transitions between them (vertical arrows) together with absorption/fluorescence spectra of Chl *a* (on the right) corresponding to these levels. For simplicity, intersystem crossing to the triplet state of Chl, as well as vibrational sublevels of the electronic energy levels of Chl are not shown. [Note: despite the use of the same notation, the electronic S_0, S_1 and S_2 states of the Chl molecules shown here are totally unrelated to the storage (S_0–S_4) states for oxidising equivalents of the $Mn_4CaO_{5/6}$ cluster in **Figure 6b**]. Modified from D. Shevela and G. Govindjee (doi.org/10.1142/10522).

to a neighbouring pigment molecule (**Figure 5a**), which can occur via two different mechanisms. If the coupling between the neighbouring pigment molecules of the LHCs is very strong, distribution of the excitation energy occurs in a *coherent* way. In such cases, the excitation energy (*exciton*) of the excited S_1 state is *delocalised* among all the pigment molecules. If the coupling between the neighbouring pigment molecules is weak, the net result is that the excitation energy gained by the absorption of a photon is localised on a single pigment molecule. In this case, the excitation energy is transferred by *hopping* from pigment to pigment.

The 'hopping' process is known as *Förster Resonance Energy Transfer* (FRET) (Şener *et al*., 2011). Here, the probability of transfer falls off quickly as the distance between the pigments increases (in many cases, the rate is proportional to R^{-6}, where R is the distance between the transition dipoles) and depends strongly on the overlap of the emission spectrum of the donor molecule and the absorption spectrum of the acceptor molecule, as well as the relative orientation of the donor and acceptor pigments. Due to favourable arrangements in light-harvesting proteins, the pigment molecules transfer their absorbed energy in the form of excitation energy to other pigment molecules until the exciton reaches the reaction centre chlorophyll *a* molecules, where the primary photochemical reaction takes place (**Figure 5a**).

Plants and many types of algae contain two types of chlorophyll molecules, *a* and *b*, which differ by a single group on one of the pyrrole rings. Because the first excited singlet state (S_1) of chlorophyll *a* is energetically lower than that of chlorophyll *b* or carotenoids, excitation energy is rapidly localised on the chlorophyll *a* molecules. Chlorophyll *b* is known to transfer excitation energy to chlorophyll *a* with 100% efficiency; thus,

excitation energy that escapes the antenna system as fluorescence comes almost entirely from chlorophyll *a*. In many plants and algae, the antenna system connected to a PSII reaction centre contains, on average, 200–250 chlorophyll and about 70 carotenoid molecules. **See also**: **Chlorophylls**

In cyanobacteria and red algae, the major light-absorbing pigments are phycobilins (phycoerythrin and phycocyanin), which are open-chain tetrapyrroles bound covalently to proteins. They also transfer excitation energy to reaction centre chlorophyll *a*, but with lower efficiency, thus showing some phycobilin fluorescence.

Carotenoids, which are linear polyenes that absorb blue and green light, serve a dual role in photosynthesis. They are important light-harvesting pigments, significantly enhancing the spectrum of visible light absorbed by the antenna system. They also protect the photosynthetic apparatus from damage under excess light, via downregulation and quenching of excited triplet states of chlorophyll to outcompete damaging side reactions with O_2.

Photosynthetic antenna systems have evolved to be highly efficient in guiding excitation energy to a reaction centre to promote primary photochemistry, rather than allowing the energy to be lost as heat or fluorescence. Measurements of photosynthesis under optimal conditions show that over 90% of absorbed photons are trapped by a reaction centre and promote charge separation. However, if a reaction centre is unable to undergo primary charge separation because the electron acceptors Q_A and Q_B are reduced (a closed reaction centre), the excitation energy is released as fluorescence or heat (**Figure 5a**). This may happen under environmental conditions that limit the rate of electron transport into the Calvin–Benson–Bassham cycle. Measurements of chlorophyll *a* fluorescence provide an effective and noninvasive method for monitoring photosynthetic performance under a wide range of conditions and environments. For further details about light absorption and excitation energy transfer in photosynthesis, see Mirkovic *et al*. (2017).

Primary Photochemistry: The Reaction Centre

As described above, the end result of the light-harvesting steps by the antenna complexes of PSII is the trapping of the excitation energy by the ensemble of two primary chlorophyll *a* (P_{D1} and P_{D2}) and two accessory chlorophyll *a* (Chl_{D1} and Chl_{D2}) molecules symmetrically arranged along the core D1 and D2 protein subunits of the PSII reaction centre (**Figure 3a**). In the reaction centre chlorophylls, the energy required to raise an electron to its higher energy level is lower than in other pigment molecules in the antenna system.

We note that in the literature these reaction centre chlorophylls are often referred to as 'P680', where 680 refers to wavelength of the red absorption maximum of these chlorophyll molecules (see **Figure 5b**). However, there is no consensus on the definition of P680. Some consider P_{D1} and P_{D2} as P680, whereas we and others include the nearby accessory Chl_{D1} and Chl_{D2} (Durrant *et al*., 1995). However, in all oxygenic photosynthetic organisms only the redox cofactors located on the D1 protein of PSII are involved in the primary charge separation.

Because the electronic energy levels of the chromophore molecules in the reaction centre core are similar, the excitation energy equilibrates rapidly (within 1 ps) between the P680 chlorophylls and the two pheophytin molecules (**Figure 1a**). The *primary charge separation* occurs from the singlet excited state of the reaction centre chlorophyll molecules, $^1P680^*$. During this process, one electron leaves one chlorophyll *a* molecule (thus forming a positively charged chlorophyll radical cation) and moves over to the pheophytin molecule, which is then reduced and forms a radical anion: $^1P680^*\ Pheo_{D1} \rightarrow P680^{\bullet+}\ Pheo_{D1}^{\bullet-}$.

The primary charge-separated state $P680^{\bullet+}\ Pheo_{D1}^{\bullet-}$ can be reached in at least two ways (Mamedov *et al*., 2015; Romero *et al*., 2017). One pathway involves excitation and charge separation within the pair $Chl_{D1}\ Pheo_{D1}$

$$(Chl_{D1}Pheo_{D1})^* \rightarrow Chl_{D1}^{\bullet+}Pheo_{D1}^{\bullet-} \rightarrow P_{D1}^{\bullet+}Pheo_{D1}^{\bullet-} \quad \text{(III)}$$

and is known as *Chl_{D1} pathway*. The other pathway proceeds through the pair $P_{D2}\ P_{D1}$

$$(P_{D2}P_{D1}Chl_{D1}Pheo_{D1})^* \rightarrow P_{D2}^{\bullet+}P_{D1}^{\bullet-} \rightarrow P_{D1}^{\bullet+}Chl_{D1}^{\bullet-} \rightarrow P_{D1}^{\bullet+}Pheo_{D1}^{\bullet-} \quad \text{(IV)}$$

and is known as *P_{D1} pathway*. Both pathways can take place in the same PSII reaction centre, and both result in the formation of the same charge-separated state $P_{D1}^{\bullet+}Pheo_{D1}^{\bullet-}$. Which pathway dominates depends on the protein conformation of the reaction centre.

The primary charge separation has a very high quantum efficiency and occurs within a few picoseconds (~3 ps), with the fastest steps occurring in 0.3 ps. The quantum efficiency of the overall reaction centre photochemistry depends on preventing the recombination of the charges. This is accomplished by the rapid (within a timescale of ~250 ps) transfer of the electron from $Pheo_{D1}^{\bullet-}$ to a tightly bound Q_A molecule that acts as a one-electron acceptor (**Figures 1c and 3a**). From $Q_A^{\bullet-}$, the electron is transferred to another, more loosely bound PQ molecule, Q_B, which acts as a two-electron acceptor. After two photochemical turnovers, Q_B becomes fully reduced and protonated, forming PQH_2. It takes about 400 µs to form Q_B^{2-} and about 1 ms to form PQH_2. PQH_2 then leaves the complex and enters the hydrophobic core of the photosynthetic membrane. The empty Q_B-binding site is then filled by an oxidised PQ molecule from the PQ pool, which takes up to 20 ms and thereby limits the turnover of PSII.

The cation radical $P680^{\bullet+}$ is the strongest oxidant known to be formed in biological reactions. The high midpoint potential of ~1.25 V enables $P680^{\bullet+}$ to sequentially withdraw electrons from the charge-accumulating Mn_4CaO_5 cluster (see **Figures 4 and 6**) via the tyrosine residue (Y_Z) of the D1 protein. The rate of electron transfer from Y_Z to $P680^{\bullet+}$ ranges from 20 ns to 35 µs, depending on the redox states of the components involved in water oxidation (**Figures 1b and 3**). The Y_Z^{ox} radical, which has a redox potential of about ~1.1 V, oxidises the Mn_4CaO_5 cluster with half times that increase with S state and range from about 0.1–2 ms, for which O_2 formation and release is the slowest step (Renger, 2012; Styring *et al*., 2012).

It is important to mention that in addition to chlorophyll *a*, other chlorophylls may be involved in primary photochemistry. For example, in the reaction centres of some cyanobacteria chlorophyll *f* is known to absorb and use far-red light (at around 727 nm) for driving charge separation (Nürnberg *et al*., 2018).

Oxidation of Water

In oxygenic photosynthesis, water is the source of electrons and protons (see reaction I) for solar energy storage by CO_2 conversion to carbohydrates. Its abundance has allowed cyanobacteria, algae, and plants to spread globally, and thereby create an atmosphere containing 21% molecular oxygen. It is remarkable that these organisms evolved the ability to oxidise water using the energy of visible light, because water is a very stable molecule.

Removing electrons one-by-one from two water molecules immediately presents two problems: One, removal of the first electron requires more energy than is contained in a photon of visible light, although removal of the second electron is readily envisioned if hydrogen peroxide can be formed (Messinger and Renger, 2008). By contrast, light-induced charge separation in PSII creates one oxidising equivalent of the same midpoint redox potential each time of approximately 1.1 V at the level of Y_Z/Y_Z^{ox} (**Figure 1c**). The second problem is high reactivity of the one-electron oxidation product, the hydroxyl radical. This problem is enhanced at low light intensities during which the redox intermediates need to be stable on the ms to seconds time scales for efficient quantum yield for O_2 production while avoiding destructive side reactions.

The Mn_4CaO_5 cluster circumvents these two problems by storing four oxidising equivalents and binding two water molecules, so that their concerted oxidation to molecular oxygen occurs only after the fourth electron is removed from the cluster. The stepwise oxidation of the Mn_4CaO_5 cluster involves sequential electron and proton removal in order to keep the midpoint redox potentials comparable for each electron abstraction (Klauss *et al*., 2012; Renger, 2012). This is schematically shown in the inner circle in **Figure 6b**, where the S_0–S_4 states (not to be confused with the S_0 ground state, and S_1 and S_2 singlet excited states of Chl, discussed above) represent the different oxidation states of the Mn_4CaO_5 cluster. As shown in the outer circle, the first three S state transitions, from S_0 up to S_3, involve Mn(III) to Mn(IV) oxidation, while in the $S_3 \rightarrow S_4$ transition, an oxygen bridge between Mn1 and Ca is oxidised (marked with X in the S_3 state of **Figure 6b**). The S_2, S_3 and S_4 states have a positive charge, because no proton is released into the bulk during the $S_1 \rightarrow S_2$ transition. Therefore, in the $S_2 \rightarrow S_3$ and $S_3 \rightarrow S_4$ transitions, a proton needs to be expelled from the Mn_4CaO_5 cluster before the unit can be oxidised by Y_Z^{ox}.

A key feature of the Mn_4CaO_5 cluster is its structural flexibility. For example, the Mn3-Mn4 distance 'shrinks' in the $S_0 \rightarrow S_1$ transition due to a deprotonation of the O5 oxo bridge. During the $S_2 \rightarrow S_3$ transition, one water molecule binds into the cluster forming a hydroxo-bridge between Mn1 and Ca, turning the Mn_4CaO_5 cluster into a Mn_4CaO_6 cluster. The conformations of the $Mn_4CaO_{5/6}$ cluster, shown in **Figure 6b,** were determined by X-ray crystallography (Kern *et al*., 2018). Data from biophysical studies indicate that additional conformations exist for each S state (see de Lichtenberg and Messinger, 2020, and references therein).

The existence of a storage unit for oxidising equivalents in PSII, the Mn_4CaO_5 cluster, was revealed in 1970 based on the period four oscillation in the O_2 yield induced by short light-flashes given to dark-adapted PSII samples (**Figure 6a**) (Joliot *et al*., 1969; Kok *et al*., 1970). As the first maximum appears after the third flash, the singly oxidised S_1 state must be the dark-stable state into which all other states (S_0, S_2 and S_3) convert after sufficiently long dark-adaptation (Messinger and Renger, 2008). The S_4 state is a transient state that is formed after the 3rd flash (see numbers on arrows in **Figure 6b**). In the S_4 state, four oxidising equivalents have been accumulated, so that the concerted oxidation of the deprotonated water molecules to molecular oxygen can occur. Therefore, the S_4 state decays to the S_0 state with the release of O_2, while the open coordination site is refilled by the binding of a new water molecule. However, after the formation of the $S_3Y_Z^{ox}$ state, a structural rearrangement must occur before O_2 can be formed (Bao and Burnap, 2015).

Although there are various options for the O—O bond formation (see **Figure 6c**), computational studies show that oxo-oxyl radical coupling (options 1 and 2) provide the lowest energy path. The main reason is that these structures provide two oxygens at a suitable distance and that the spin coupling provides electrons with opposite spins for the formation of the initial O—O bond (Li and Siegbahn, 2015; Siegbahn, 2009).

The H-bonding networks provided by the water molecules and specific amino acids in the channels connecting the Mn_4CaO_5 cluster with the lumen are crucial for proton removal from the active site (see **Figure 3b and 4a**). Alterations in these channels, specifically the Cl1 channel, lead to slowing or even inhibition of the $S_2 \rightarrow S_3$ and/or the $S_3 \rightarrow S_4 \rightarrow S_0$ transitions. In addition, these channels supply water molecules to the Mn_4CaO_5 cluster.

The Ca ion in the Mn_4CaO_5 cluster is of central importance because: (1) it likely contributes to tuning the redox potentials of the Mn ions (Tsui and Agapie, 2013), (2) it coordinates a water molecule (W4; **Figure 4a**) that hydrogen bonds Y_Z (Tyr_Z) and thereby stabilises the Y_Z position, (3) it likely facilitates water binding to Mn in the $S_2 \rightarrow S_3$ and $S_3 \rightarrow S_4 \rightarrow S_0$ transitions, and (4) Ca coordinates, in the S_3 and S_4 states, the two oxygens that likely form the O—O bond (Cox and Messinger, 2013; de Lichtenberg and Messinger, 2020). Similarly, the two water molecules on Mn4 are crucial for proton removal from the cluster during the S state transitions and may also be involved in providing new substrate water molecules.

The Mn_4CaO_5 cluster is assembled into apo-PSII by light-induced oxidation of Mn^{2+} ions from solution. This is a highly complex process that in its first steps has a very low quantum yield due to protein conformational changes (Avramov *et al*., 2020; Cheah *et al*., 2020).

Translating the principles of photosynthetic water oxidation into synthetic catalysts is an active area of research focusing on producing highly efficient water oxidation catalysts from abundant first-row transition metals such as Mn (Roger *et al*., 2017; Zhang and Sun, 2019).

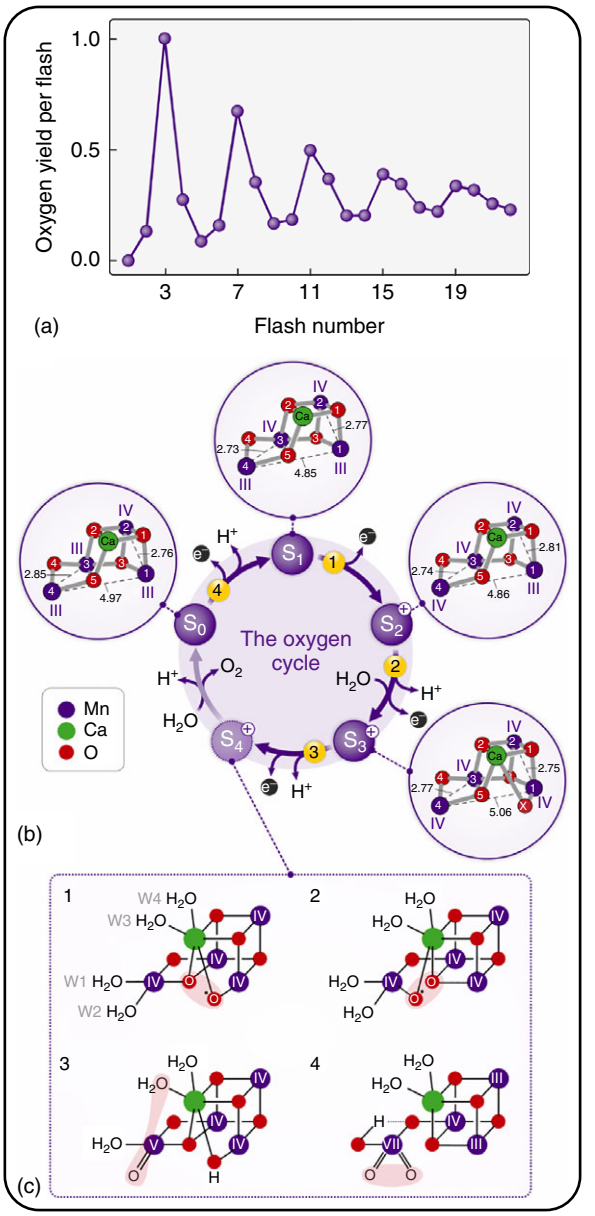

Figure 6 The 'oxygen cycle' of the Mn_4CaO_5 cluster and the structures of its redox state intermediates in photosystem II (PSII). (a) Flash-induced oxygen yields from dark-adapted PSII samples as a function of flash number; similar data were originally reported by Joliot *et al.* (1969). (b) Oxygen cycle (also referred to as 'Kok's clock' or the S state cycle; see Kok *et al.*, 1970), with flash-induced electron abstraction by $P680^{\bullet+}$ via Y_Z^{ox}, proton release, water binding and accumulation of a positive charge (+). The outer circles display the structures of the $Mn_4CaO_{5/6}$ cluster in each stable S state as determined by X-ray diffraction (Kern *et al.*, 2018). The numbers on the arrows indicate the number of flashes given to a dark-adapted PSII sample. (c) Simplified structures for four suggested pathways for the O—O bond formation in the S_4 state of the $Mn_4CaO_{5/6}$ cluster in PSII: *1* and *2* show two versions of oxo-oxyl radical coupling between O5 and OX/O6 (Li and Siegbahn, 2015, Siegbahn, 2009), which are presently the best-supported mechanisms; *3* represents a nucleophilic attack of Ca-bound W3 onto Mn-bound W2, which is assumed to be a Mn(V)=O or Mn(IV)-$O^{\bullet}$ in the S_4 state (McEvoy and Brudvig, 2006); and *4* represents geminal coupling of two-terminal oxo ligands at a Mn(VII) species formed by disproportionation of the Mn oxidation states in the S_4 state (Zhang and Sun, 2018). In addition (not shown), O—O bond formation in the S_3 state is discussed (Corry and O'Malley, 2020; Renger, 2012).

Reduction of Plastoquinone: The Two-electron Gate

PQ plays a key role in photosynthesis by linking electron transport to proton transfer across the photosynthetic membrane. In the PSII complex, two PQ molecules work in tandem, with one molecule permanently bound at the Q_A site, and another molecule bound transiently at the Q_B site. Once PQ at the Q_B site has been fully reduced by the addition of two electrons and two protons, the reduced form (PQH_2) is released into the photosynthetic

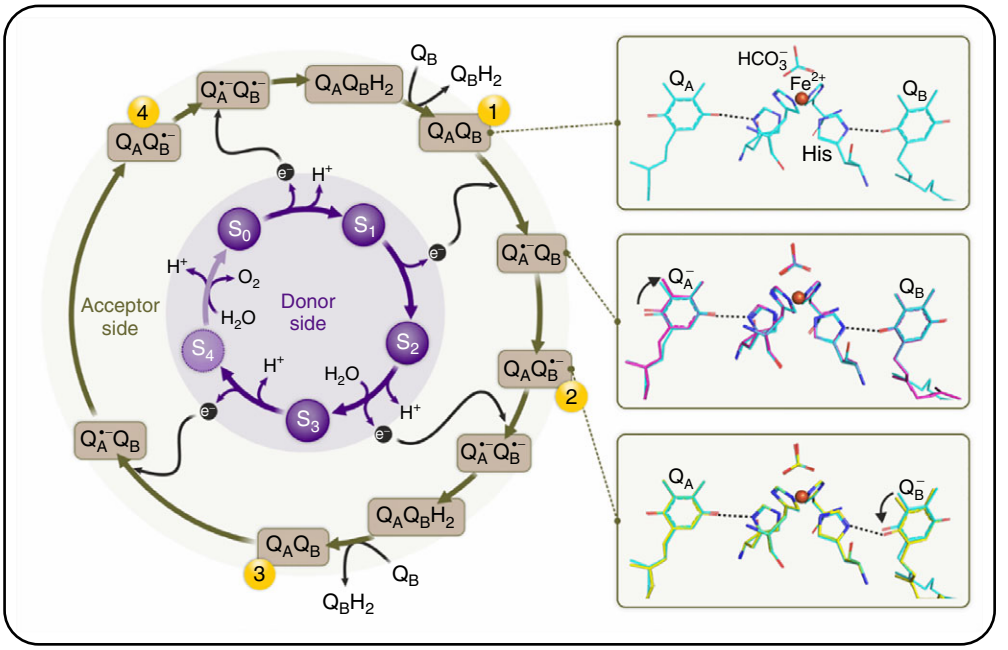

Figure 7 Steps in the two-electron reduction of plastoquinone at the acceptor side of Photosystem II (PSII), which is also known as the two-electron gate (Velthuys and Amesz, 1974 and Bouges-Bocquet, 1973). The inner circle shows its relationship with the oxygen cycle at the donor side of dark-adapted PSII samples with fully oxidised Q_A and Q_B. Structural changes at the acceptor side are indicated for the Q_AQ_B (dark adapted), $Q_A^{\bullet-}Q_B$ (50 µs after 1st flash), and $Q_AQ_B^{\bullet-}$ (400 µs after 1st flash) states based on the room temperature time-resolved diffraction data in Kern *et al.* (2018) and Ibrahim *et al.* (2020). The numbers on yellow spheres indicate when in the cycle the respective flashes are given. Structural figures were generated by using coordinates of the PDB codes 6W1O (Q_AQ_B), 6W1R ($Q_A^{\bullet-}$), and 6W1P ($Q_B^{\bullet-}$).

membrane. The reduction of PQ at the Q_B site is known as the two-electron gate because two electrons, and, therefore, two photochemical reactions are required for the formation and release of PQH_2 (Bouges-Bocquet, 1973; Müh *et al.*, 2012; Velthuys and Amesz, 1974). The Q_B site of PSII is of particular interest because some herbicides used in agriculture (e.g. atrazine and terbutryn) inhibit photosynthesis by binding at the Q_B site.

A nonheme iron, which is coordinated by four histidine residues (two from subunit D1 and two from subunit D2) is located at the centre between the two quinones. The two additional ligation sites of the Fe bind a bicarbonate ion as a bidentate ligand (Umena *et al.*, 2011). This correlates with previous evidence that bicarbonate/carbonate ions play a role in formation of Q_B^- and its subsequent protonation (see discussion below). Recent room temperature structural studies enable visualisation of the formation of the reduced PQ species (Ibrahim *et al.*, 2020; Kern *et al.*, 2018). At 50 µs after the formation of $Q_A^{\bullet-}$, induced by a light flash, a small rotation of the ring of the Q_A group is observed (**Figure 7**). This rotation is reversed and a similar rotation of the Q_B head group is seen 400 µs after the flash, indicating the formation of the $Q_A/Q_B^{\bullet-}$ state that occurs within 200–300 µs. In this state, $Q_B^{\bullet-}$ is likely stabilised by protonation of a nearby amino acid side chain. After a subsequent charge separation, another electron is transferred – this time from $Q_A^{\bullet-}$ to $Q_B^{\bullet-}$. This step is slower due to the negative charge of $Q_B^{\bullet-}$ and occurs within 600–700 µs, most likely via a coupled proton-electron transfer step, producing the state Q_A/Q_BH^-. Q_BH^- takes up another proton from the outer water phase via a network of proton-transferring amino acid side chains, producing PQH_2. Upon full reduction, PQH_2 debinds from the Q_B site, migrates through a hydrophobic quinone exchange cavity within the protein complex and enters the hydrophobic core of the photosynthetic membrane (Müh *et al.*, 2012). The reduction cycle is repeated by binding of a PQ molecule from the quinone exchange cavity.

Role of bicarbonate ions in light-induced reactions of photosystem II

Research over the last five decades has revealed that bicarbonate ions (HCO_3^-, hydrogen carbonate) support light-induced electron and proton transfer reactions of PSII (Shevela *et al.* 2012). As described above, bicarbonate is a bidentate ligand to the nonheme iron between Q_A and Q_B in PSII reaction centres (see Figures **3a** and **7**) of all oxygenic photosynthetic organisms. This is not the case in the reaction centres of anoxygenic photosynthetic bacteria, indicating that bicarbonate plays a role only in oxygenic photosynthesis. It stabilises the Q_A–Fe^{2+}–Q_B structure of the PSII reaction centre, allowing protonation of $Q_B^{\bullet-}$ via certain amino acids around this site and, thereby, accelerates electron transfer from the reduced Q_A ($Q_A^{\bullet-}$) to Q_B ($Q_B^{\bullet-}$). Light-induced formation of $Q_A^{\bullet-}$ weakens HCO_3^- binding, which can lead to loss of HCO_3^- from its binding site, especially when the concentration of HCO_3^-/CO_2 becomes low in the chloroplast or

cell. This finding indicates that the absence of bicarbonate might downregulate the electron transfer between Q_A and Q_B and the Q_BH_2 exchange with the PQ pool, thus lowering the risk for over-reduction of the PQ pool when inorganic carbon becomes limiting for electron flow. In addition, bicarbonate has a protective function for PSII as its release tunes the redox potentials of cofactors in a way that the formation of long-lived radical states during charge recombination reactions is prevented. On the water-splitting side of PS II, easily exchangeable (mobile) HCO_3^- ions enhance the water-oxidising activity by helping to shuttle protons produced during water-splitting into the lumen. Thus, both water oxidation and PQ reduction of PSII are downregulated at low dissolved inorganic carbon (HCO_3^-/CO_2) levels, which lowers the risk of PSII photodamage and minimises the reductive pressure in the electron transport chain (Shevela *et al*., 2020). Additionally, bicarbonate is also thought to be a cofactor during the photo-assembly of the Mn_4CaO_5 cluster (see Avramov *et al*., 2020 and references therein).

Photosystem II contributes to the transmembrane proton electrochemical potential difference that drives ATP synthesis

The production of ATP in photosynthesis depends on the conversion of energy, generated by the two photosystems, into a 'transmembrane proton electrochemical potential gradient' (also known as *the proton motive force*; *pmf*), which is made up of both a pH gradient (ΔpH) and an electrical potential gradient (ΔΨ) across the photosynthetic membrane (Mitchell, 2011). PSII contributes to the generation of the *pmf* by the release of four protons into the lumen (the *p* side of the thylakoid membrane) associated with the water splitting, and by the uptake of protons from the stromal/cytoplasmic side of thylakoid membrane (the *n* side) associated with the reduction of PQ (**Figure 1b**). The latter reaction is the first step of the proton-transporting mechanism that is completed by the oxidation of PQH_2 by the Cyt b_6f complex (Sarewicz *et al*., 2021). Thus, consecutive reduction and oxidation of two PQ molecules lead to the transfer of another four protons (in addition to four protons from water-splitting reaction) from the stroma/cytoplasm to the lumen. In addition to the ΔpH that is built up in this way, an electrical potential gradient (ΔΨ) is also created across the thylakoid membrane due to electron transfer through the PSII reaction centre from water (luminal side) to PQ (stromal/cytoplasmic side). It appears that the elevated ΔΨ component of the generated *pmf* can alter recombination reactions of PSII (Davis *et al*., 2016), leading to increased production of harmful $^1O_2$ species, which subsequently cause photodamage to PSII, thus-limiting photosynthetic productivity. **See also**: **Mitchell, Peter Dennis**; **Oxidative Phosphorylation**; **Photosynthesis: Light Reactions**

Concluding Remarks

PSII is able to collect visible light from the sun and use the energy to oxidise water and reduce PQ. Over the past 3 billion years, this process has produced the oxygen we breathe and has contributed reducing equivalents needed for storing the captured solar energy in the bonds of carbohydrates, which provide the building blocks for nearly all life on Earth, including the biomass that has been transformed into fossil fuels. We hope that this description of our current understanding of structure and function of this remarkable protein complex will inspire research designed to use solar energy to advance food production, via engineered photosynthetic organisms, and to mitigate global climate change by replacing fossil fuels, the product of past photosynthesis, by carbon-neutral solar fuels produced via artificial and modified biological systems.

Glossary

Chloroplast Subcellular organelle in plants and algae in which photosynthesis occurs.

Cytochrome c550 A heme-containing protein associated with photosystem II, often found in cyanobacteria but not in eukaryotic organisms.

Cytochrome b559 A heme-containing protein that is an integral part of photosystem II complexes.

Lumen The aqueous phase enclosed by the thylakoid membrane (also referred to as the inner water phase).

Oxidation The removal of one or more electrons from a molecule, ion or complex; in some oxidation reactions, protons are released as well.

Plastoquinone A small organic molecule involved in electron and proton transfer in photosynthesis.

Reaction centre A pigment–protein complex that converts light energy or excitation energy into chemical energy.

Reduction The addition of one or more electrons to a molecule, ion or complex; in some reduction reactions, protons are taken up as well.

Stroma or cytoplasm The water (or aqueous) phase of the chloroplast (stroma) or cyanobacterium (cytoplasm) that is located outside the vesicle formed by the thylakoid membrane. The CO_2 reduction (the Calvin–Benson–Bassham) cycle enzymes are located in the stroma.

Thylakoid or photosynthetic membrane A vesicular membrane that encloses an inner aqueous phase (lumen) and contains the protein complexes for light-driven electron transport and ATP synthesis.

References

Avramov AP, Hwang HJ and Burnap RL (2020) The role of Ca^{2+} and protein scaffolding in the formation of nature's water oxidizing complex. *Proceedings of the National Academy of Sciences of the United States of America* **117**: 28036–28045.

Bao H and Burnap RL (2015) Structural rearrangements preceding dioxygen formation by the water oxidation complex of photosystem II. *Proceedings of the National Academy of Sciences of the United States of America* **112**: E6139–E6147.

Blankenship RE, Tiede DM, Barber J, *et al*. (2011) Comparing photosynthetic and photovoltaic efficiencies and recognizing the potential for improvement. *Science* **332**: 805–809.

Bouges-Bocquet B (1973) Limiting steps in photosystem II and water decomposition in *Chlorella* and spinach chloroplasts. *Biochimica et Biophysica Acta* **292**: 772–785.

Catling DC and Zahnle KJ (2020) The Archean atmosphere. *Science Advances* **6**: eaax1420.

Cheah MH, Zhang M, Shevela D, *et al*. (2020) Assessment of the manganese cluster's oxidation state via photoactivation of photosystem II microcrystals. *Proceedings of the National Academy of Sciences of the United States of America* **117**: 141–145.

Corry TA and O'Malley PJ (2020) Electronic–level view of O–O bond formation in Nature's water oxidizing complex. *The Journal of Physical Chemistry Letters* **11**: 4221–4225.

Cox N and Messinger J (2013) Reflections on substrate water and dioxygen formation. *Biochimica et Biophysica Acta - Bioenergetics* **1827**: 1020–1030.

Dau H and Zaharieva I (2009) Principles, efficiency, and blueprint character of solar-energy conversion in photosynthetic water oxidation. *Accounts of Chemical Research* **42**: 1861–1870.

Davis GA, Kanazawa A, Schöttler MA, *et al*. (2016) Limitations to photosynthesis by proton motive force-induced photosystem II photodamage. *eLife* **5**: e16921.

Durrant JR, Klug DR, Kwa SLS, *et al*. (1995) A multimer model for P680, the primary electron-donor of photosystem II. *Proceedings of the National Academy of Sciences of the United States of America* **92**: 4798–4802.

Govindjee G, Shevela D and Björn LO (2017) Evolution of the Z-scheme of photosynthesis: a perspective. *Photosynthesis Research* **133**: 5–15.

Green BR (2019) What happened to the phycobilisome? *Biomolecules* **9**: 748.

Ho FM (2012) Substrate and product channels in photosystem II. In: Wydrzynski TJ and Hillier W (eds) *Molecular Solar Fuels*, pp 208–248. RCS Publishing: Cambridge.

Ibrahim M, Fransson T, Chatterjee R, *et al*. (2020) Untangling the sequence of events during the $S_2 \rightarrow S_3$ transition in photosystem II and implications for the water oxidation mechanism. *Proceedings of the National Academy of Sciences of the United States of America* **117**: 12624–12635.

Joliot P, Barbieri G and Chabaud R (1969) Un nouveau modele des centres photochimiques du systeme II. *Photochemistry and Photobiology* **10**: 309–329.

Kern J, Chatterjee R, Young ID, *et al*. (2018) Structures of the intermediates of Kok's photosynthetic water oxidation clock. *Nature* **563**: 421–425.

Klauss A, Haumann M and Dau H (2012) Alternating electron and proton transfer steps in photosynthetic water oxidation. *Proceedings of the National Academy of Sciences of the United States of America* **109**: 16035–16040.

Kok B, Forbush B and McGloin M (1970) Cooperation of charges in photosynthetic O_2 evolution. *Photochemistry and Photobiology* **11**: 457–476.

Lee W-J and Whitmarsh J (1989) Photosynthetic apparatus of pea thylakoid membranes. *Plant Physiology* **89**: 932–940.

Li X and Siegbahn PEM (2015) Alternative mechanisms for O_2 release and O–O bond formation in the oxygen evolving complex of photosystem II. *Physical Chemistry Chemical Physics* **17**: 12168–12174.

de Lichtenberg C and Messinger J (2020) Substrate water exchange in the S_2 state of photosystem II is dependent on the conformation of the Mn_4Ca cluster. *Physical Chemistry Chemical Physics* **22**: 12894–12908.

Mamedov M, Govindjee G, Nadtochenko V and Semenov A (2015) Primary electron transfer processes in photosynthetic reaction centers from oxygenic organisms. *Photosynthesis Research* **125**: 51–63.

McEvoy JP and Brudvig GW (2006) Water-splitting chemistry of photosystem II. *Chemical Reviews* **106**: 4455–4483.

Messinger J and Renger G (2008) Photosynthetic water splitting. In: Renger G (ed.) Primary Processes of Photosynthesis*, Part 2, Principles and Apparatus*, vol. **9**, pp 291–351. RSC Publishing: Cambridge.

Mirkovic T, Ostroumov EE, Anna JM, *et al*. (2017) Light absorption and energy transfer in the antenna complexes of photosynthetic organisms. *Chemical Reviews* **117**: 249–293.

Mitchell P (2011) Chemiosmotic coupling in oxidative and photosynthetic phosphorylation. *Biochimica et Biophysica Acta - Bioenergetics* **1807**: 1507–1538.

Moser CC, Keske JM, Warncke K, *et al*. (1992) Nature of biological electron-transfer. *Nature* **355**: 796–802.

Müh F, Glöckner C, Hellmich J and Zouni A (2012) Light-induced quinone reduction in photosystem II. *Biochimica et Biophysica Acta - Bioenergetics* **1817**: 44–65.

Müh F and Zouni A (2020) Structural basis of light-harvesting in the photosystem II core complex. *Protein Science* **29**: 1090–1119.

Nürnberg DJ, Morton J, Santabarbara S, *et al*. (2018) Photochemistry beyond the red limit in chlorophyll f–containing photosystems. *Science* **360**: 1210–1213.

Ort DR, Merchant SS, Alric J, *et al*. (2015) Redesigning photosynthesis to sustainably meet global food and bioenergy demand. *Proceedings of the National Academy of Sciences of the United States of America* **112**: 8529–8536.

Renger G and Renger T (2008) Photosystem II: the machinery of photosynthetic water splitting. *Photosynthesis Research* **98**: 53–80.

Renger G (2012) Mechanism of light induced water splitting in Photosystem II of oxygen evolving photosynthetic organisms. *Biochimica et Biophysica Acta - Bioenergetics* **1817**: 1164–1176.

Roger I, Shipman MA and Symes MD (2017) Earth-abundant catalysts for electrochemical and photoelectrochemical water splitting. *Nature Reviews Chemistry* **1**: 0003.

Romero E, Novoderezhkin VI and van Grondelle R (2017) Quantum design of photosynthesis for bio-inspired solar-energy conversion. *Nature* **543**: 355–365.

Roose JL, Frankel LK, Mummadisetti MP and Bricker TM (2016) The extrinsic proteins of photosystem II: update. *Planta* **243**: 889–908.

Sarewicz M, Pintscher S, Pietras R, *et al*. (2021) Catalytic reactions and energy conservation in the cytochrome bc_1 and b_6f complexes of energy-transducing membranes. *Chemical Reviews* **121**: 2020–2108.

Şener M, Strümpfer J, Hsin J, *et al*. (2011) Förster energy transfer theory as reflected in the structures of photosynthetic light-harvesting systems. *ChemPhysChem* **12**: 518–531.

Shevela D, Eaton-Rye JJ, Shen J-R and Govindjee G (2012) Photosystem II and the unique role of bicarbonate: a historical perspective. *Biochimica et Biophysica Acta - Bioenergetics* **1817**: 1134–1151.

Shevela D, Do H-N, Fantuzzi A, *et al*. (2020) Bicarbonate-mediated CO_2 formation on both sides of photosystem II. *Biochemistry* **59**: 2442–2449.

Shi L-X, Hall M, Funk C and Schröder WP (2012) Photosystem II, a growing complex: updates on newly discovered components and low molecular mass proteins. *Biochimica et Biophysica Acta - Bioenergetics* **1817**: 13–25.

Siegbahn PEM (2009) Structures and energetics for O_2 formation in photosystem II. *Accounts of Chemical Research* **42**: 1871–1880.

Styring S, Sjöholm J and Mamedov F (2012) Two tyrosines that changed the world: Interfacing the oxidizing power of photochemistry to water splitting in photosystem II. *Biochimica et Biophysica Acta - Bioenergetics* **1817**: 76–87.

Su X, Ma J, Wei X, *et al*. (2017) Structure and assembly mechanism of plant $C_2S_2M_2$-type PSII-LHCII supercomplex. *Science* **357**: 815–820.

Tsui EY and Agapie T (2013) Reduction potentials of heterometallic manganese–oxido cubane complexes modulated by redox-inactive metals. *Proceedings of the National Academy of Sciences of the United States of America* **110**: 10084–10088.

Umena Y, Kawakami K, Shen J-R and Kamiya N (2011) Crystal structure of oxygen-evolving photosystem II at a resolution of 1.9 Å. *Nature* **473**: 55–60.

Velthuys BR and Amesz J (1974) Charge accumulation at the reducing side of system 2 of photosynthesis. *Biochimica et Biophysica Acta* **333**: 85–94.

Zhang B and Sun L (2018) Why nature chose the Mn_4CaO_5 cluster as water-splitting catalyst in photosystem II: a new hypothesis for the mechanism of O–O bond formation. *Dalton Transactions* **47**: 14381–14387.

Zhang B and Sun L (2019) Artificial photosynthesis: opportunities and challenges of molecular catalysts. *Chemical Society Reviews* **48**: 2216–2264.

Further Reading

Blankenship RE (2021) *Molecular Mechanisms of Photosynthesis*, 3rd edn. Wiley-Blackwell: Oxford.

Cramer WA and Knaff DB (1991) *Energy Transduction in Biological Membranes: A Textbook of Bioenergetics*. Springer: New York, NY.

Demmig-Adams B, Garab G, Adams IIIWW and Govindjee G (eds) (2014) Non-Photochemical Quenching and Energy Dissipation in Plants, Algae and Cyanobacteria, *Advances in Photosynthesis and Respiration*, vol. **40**. Springer: Dordrecht.

Lane N (2003) *Oxygen – The Molecule that Made the World*. Oxford University Press: Oxford.

MacKay DJC (2009) *Sustainable Energy – Without the Hot Air*. UIT Cambridge Ltd: Cambridge.

Papageorgiou GC and Govindjee G (eds) (2004) Chlorophyll a Fluorescence: A Signature of Photosynthesis, *Advances in Photosynthesis and Respiration*, vol. **19**. Springer: Dordrecht.

Renger G (2008) *Primary Processes of Photosynthesis: Principles and Apparatus*. RSC Publishing: Cambridge.

Shevela D, Björn LO and Govindjee G (2018) *Photosynthesis: Solar Energy for Life*. World Scientific: New Jersey.

Wydrzynski T and Satoh K (eds) (2005) Photosystem II. The Light-Driven Water:Plastoquinone Oxidoreductase, *Advances in Photosynthesis and Respiration*, vol. **22**. Springer: Dordrecht.

Zhu X-G, Long SP and Ort DR (2008) What is the maximum efficiency with which photosynthesis can convert solar energy into biomass? *Current Opinion in Biotechnology* **19**: 153–159.